

Gold Nanorod, an Optical Probe to Track HIV Infection

Santosh Kumar

Department of Applied Sciences, Radha Govind Engineering College, Meerut, India
Email: bhu.santosh71@gmail.com

Received August 9, 2011; revised September 6, 2011; accepted October 1, 2011

ABSTRACT

Infectious diseases caused by the human immunodeficiency virus (HIV) remain the leading killers of human beings worldwide, and function to destabilize societies in Africa, Asia and the Middle East. Driven by the need to detect the presence of HIV viral sequence, here we demonstrate that the second order nonlinear optical (NLO) properties of gold nanorods can be used for screening HIV-1 viral DNA sequence without any modification, with good sensitivity (100 pico-molar) and selectivity (single base pair mismatch). The hyper Rayleigh Scattering (HRS) intensity increases 58 times when label-free 145-mer, ss-*gag* gene DNA, was hybridized with 100 pM target DNA. The mechanism of HRS intensity change has been discussed with experimental evidence for higher multipolar contribution to the NLO response of gold nanorods.

Keywords: HRS; Nanomaterial; HIV

1. Introduction

Infectious diseases remain the leading killers of human civilization worldwide, and function to destabilize societies in Africa, Asia and the Middle East. Acquired immunodeficiency syndrome (AIDS) a degenerative disease of the immune system is caused by the human immunodeficiency virus (HIV). The current statistics for global HIV/AIDS are staggering, as an estimated 45 million people worldwide are ailing with HIV/AIDS. Diagnosis of human immunodeficiency virus (HIV) infection is commonly based on the detection of antibodies to HIV, but specific anti-HIV antibodies, usually occurs 3 to 8 weeks after the infectious contact and 5 to 10 days after the onset of symptoms associated with early infection. Despite infection of nearly 60 million individuals worldwide with HIV, fewer than 1000 cases have been diagnosed in the first month of infection, primarily because of the lack of a specific and recognizable acute retroviral syndrome. There is need for a direct DNA-based test, which detects the presence of HIV viral sequence. The nanoscience revolution that sprouted throughout the 1990s is having great impact in current and future DNA detection technology around the world [1-12]. The increasing availability of nanostructures with highly controlled optical properties in the nanometer size range has created widespread interest in their use in biotechnological system for diagnostic application and biological imaging. Nano-surface fluorescence energy transfer (NSET) [13-16] and Surface enhanced Raman spectroscopic technique (SERS) [17-20] have been shown to be highly

promising technologies to detect DNA present at very low concentrations. But these assays identify specific sequence through hybridization of an immobilized probe to the target analyte after the latter has been modified with a covalently linked label such as a fluorescent or Raman tag. Necessity of tagging makes it difficult to use SERS and Fluorescence Resonance Energy Transfer (FRET) techniques as biosensors for real life. Diagnostic of oligonucleotide sequence using unmodified DNA remains attractive due to simple sample preparation, decrease assay cost and the elimination of potential artifacts from modification. Driven by the need, in this article, we demonstrate the second order nonlinear optical (NLO) properties [21-27] of gold nanomaterial can be used for screening HIV DNA without any modification, with excellent sensitivity (100 pico-molar) and selectivity (single base pair mismatch).

Gold nanosystems have created widespread interest in their use in biotechnological systems for diagnostic applications and biological imaging because of their shape and size-dependent optical properties, whose origin is localized surface plasmon resonance (LSPR) and ease of bioconjugation and potential noncytotoxicity [1-7]. Conjugates of gold nanoparticles with oligonucleotides are of great current interest [1-20] because of the potential use of the programmability of DNA base pairing to organize nano-crystal in space and the multiple ways of providing a signature for the detection of precise DNA sequence. After a pioneering work by Mirkin *et al.* [28] several groups [1-20] are working in this area using different methods. The absorption spectra of rod-shaped gold nan-

oparticles, known as gold nanorods, exhibits two surface plasmon absorption bands [8-12]. A strong long wavelength band in the near-infrared region due to the longitudinal oscillation of the conduction band electrons, and a weak short wavelength band around 520 nm due to the transverse electronic oscillations. The longitudinal absorption band is very sensitive to the aspect ratio and by increasing the aspect ratio (length divided by width), the longitudinal absorption maximum shifts to longer wavelength with an increase in the absorption intensity. Because of the enhanced surface electric field upon surface plasmon excitation, gold nanorods absorb and will be able to scatter electromagnetic radiation strongly. This unique optical property of gold nanorods opens up fascinating applications in developing biological and chemical sensors. Gold nanorods (GNRs) should provide several advantages over spherical gold nanoparticles for biological sensing and those are 1) the LSPR properties of GNRs can be tuned by adjusting their aspect ratio from the visible to the NIR region, and 2) the longitudinal absorption band is extremely sensitive to changes in the dielectric properties of the surroundings including solvents, adsorbates, and the interparticle distance of the GNRs. In this manuscript, we reported extremely high second order nonlinear optical properties (NLO) from gold nanorods due to the presence of multipole moments from the size and retardation effects. NLO properties have been monitored using hyper-Rayleigh scattering (HRS) technique [6,21-27]. Using this enhanced, sensitive, and tunable optical scattering properties, here we have shown that the hyper-Rayleigh scattering (HRS) technique [6,21-27] which has emerged over the past decade as a powerful method to determine the microscopic non-linear optical (NLO) properties of species in solution, can be used to achieve detection of HIV-DNA with excellent sensitivity (100 pM) and selectivity.

2. Experimental Section

2.1. Synthesis and Characterization of Gold Nanorods

Gold nanorods were synthesized using a seed-mediated, surfactant-assisted growth method in a two-step procedure [8-12,29-34]. Colloidal gold seeds (~1.5 nm diameter) were first prepared by mixing aqueous solutions of hexadecyltrimethylammonium bromide (CTAB, 0.1 M, 4.75 mL) and hydrogen tetrachloroaurate(III) hydrate (0.01 M, 0.2 mL). An aqueous solution of sodium borohydride (0.01 M, 0.6mL) was then added. The colloidal gold seeds were then injected into an aqueous growth solution of CTAB (0.1 M, 4.75 mL), silver nitrate (0.01 M, varying amounts of silver between 20 and 120 mL depending on desired nanorod aspect ratio), hydrogen tetrachloroaurate(III) hydrate (0.01 M, 0.2 mL), and ascor-

bic acid (0.1 M, 0.032 mL). Nanorods were purified by several cycles of suspension in ultrapure water, followed by centrifugation. Nanorods were isolated in the precipitate, and excess CTAB was removed in the supernatant and characterized by TEM and absorption spectroscopy (as shown in **Figure 1**).

2.2. Preparation of DNA Gold Nanorod Conjugates

The nanorods prepared by above methods were capped with a bilayer of cetyltrimethylammonium bromide (CTAB), which is positively charged. The positively charged surface of the nanorods was changed to a negatively charged surface by exposing the nanoparticles to poly (styrene-sulfonate) (PSS) polyelectrolyte solution. The extra PSS in solution was separated by centrifuging the rod solution at 10,000 rpm, and the pellet was redispersed in *N*-(2-hydroxyethyl)piperazine-*N'*-2-ethanesulfonic acid (HEPES) solution. The PSS-capped nanorods were then mixed with probe DNA solution that was diluted in buffer and allowed to react for 20 min. The probe DNA is probably bound to the PSS-coated nanorods by a mechanism similar to that used for binding DNA to nanospheres, *i.e.*, by electrostatic physisorption interaction [14,16,35,36]. Direct evidence for the preferential interaction between dye-tagged ssDNA and gold nanoparticles is illustrated in **Figure 2**. Our experimental data show quenching of the dye photoluminescence from dye-tagged ssDNA and enhancement of resonant Raman scattering from the dye. Fluorescence emitted from AlexaFluor 647 (AF647) modified ssDNA (AF647-5'-AGAAGATATTTGGAATAACATGACCTGGATGCA-3') was quenched more than 95% by gold nanorod as shown in **Figure 2(a)**. Several order of magnitudes surface-enhanced resonant Raman scattering (SERRS) signal enhancement were observed (as shown in **Figure 2(b)**) from rhodamine 6G tagged ssDNA (Rh6G -5'-AGAAGATATTTGGAATAACATGACCTGGATGCA-3') adsorbed on gold nanorods. The Raman modes at 234, 253, 273 and 371 cm^{-1} are N-C-C bending modes of ethylamine group of the Rh6G ring and the strong Raman modes at 613, 777, 1182, 1347 and 1366 cm^{-1} are due to C-C-C ring in-plan bending, C-H out-of-plan bending, C-C stretching and C-N stretching.

Since certain regions of the *gag* gene, such as p24, are highly conserved among human immunodeficiency virus (HIV) isolates, many therapeutic strategies have been directed at *gag* gene targets. We therefore used a segment of HIV *gag* gene sequence as a target DNA. To demonstrate that HRS assay can be used for HIV-DNA detection, we used initially a partial sequence of the HIV-1 *gag*-gene, 5'-AGAAGATATTTGGAATAACATGACCTGGATGCA-3' as the probe. Then to understand the capability of our HRS assay for longer DNA sequences we have used

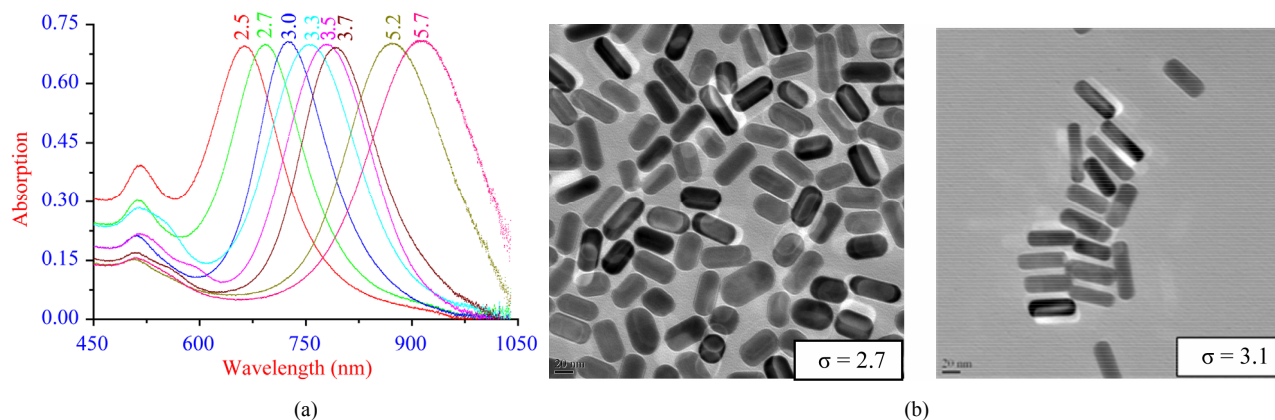


Figure 1. (a) Extinction profile of Au nanorods with aspect ratios from 2.5 to 5.7. The strong long wavelength band in the near-infrared region ($\lambda_{LPR} = 600 - 950$ nm) is due to the longitudinal oscillation of the conduction band electrons. The short wavelength peak ($\lambda \approx 520$ nm) is from the nanorods' transverse plasmon mode; (b) TEM image of nanorods of average aspect ratios ($\sigma \approx 2.7$ and 3.1).

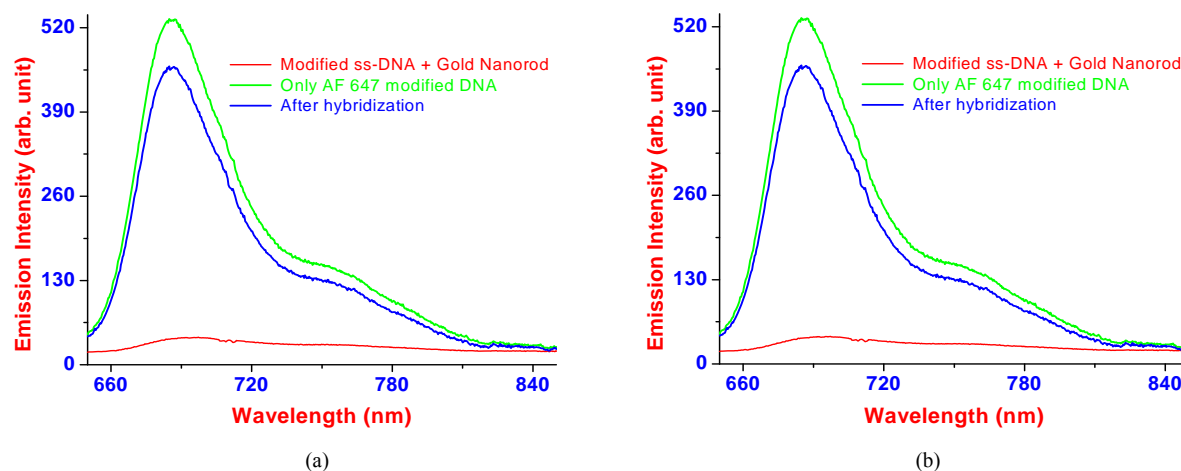


Figure 2. Shows evidences for preferential adsorption of ssDNA on gold nanorods. (a) Fluorescence emitted from AlexaFluor 647 (AF647) modified to ssDNA (AF647-5'-AGAAGATATTTGGAATAACATGACCTGGATGCA-3') was quenched more than 95% by gold nanorods. Upon hybridization, the double-strand (ds) DNA is no longer adsorbed onto the gold nanorods and the fluorescence of the attached dye persists; (b) Surface-enhanced resonant Raman scattering (SERRS) from rhodamine 6G tagged ssDNA (Rh6G -5'-AGAAGATATTTGGAATAACATGACCTGGATGCA-3') with and without gold nanorods.

86, 115 and 142-bp fragment from the *gag* region. Oligonucleotides with different chain lengths, and its complement and non-complement (one and two base pair mismatch) were purchased from the Midland Certified Reagent Company. Hybridization of the probe and the target was conducted for 5 minutes in phosphate buffer solution with 0.3 M NaCl for few minutes at room temperature. An aliquot of the hybridization solution was added to 1 ml of the gold nanorod solution. 1 ml of phosphate buffer was added immediately to the same solution.

2.3. Hyper Rayleigh Scattering Spectroscopy

The HRS technique is based on light scattering. The intensity of the Rayleigh scattering is linearly dependent on the number density and the impinging laser intensity, and

quadratically on the linear polarizability α . The HRS or nonlinear light scattering can be observed from fluctuations in symmetry, caused by rotational fluctuations. This is a second harmonic generation experiment in which the light is scattered in all directions rather than as a narrow coherent beam. The technique can be easily applied to study a very wide range of materials because electrostatic fields and phase matching are not required [6,21-26,37-40]. Other advantages are that the polarization analysis gives information about the tensor properties, and spectral analysis of the scattered light gives information about the dynamics. We have monitored the second order NLO properties using HRS technique. The HRS or nonlinear light scattering can be observed from fluctuations in symmetry, caused by rotational fluctuations. Scattering by a fundamental laser beam can be detected at the se-

cond harmonic wavelength. This is a second harmonic generation experiment in which the light is scattered in all directions rather than as a narrow coherent beam. For the HRS experiment, we have used a mode-locked Ti: sapphire laser delivering at fundamental wavelength of 860 nm with a pulse duration of about 150 fs at a repetition rate of 80 MHz. We performed TEM data (as shown in **Figure 1(b)**) before and after exposure of about 5 minutes to the laser and we have not noted any photo-thermal damage of gold nanorods within our HRS data collecting time. After passing through a low-pass filter, fundamental beam of about 100 mW was focused into quartz cell containing the aqueous solutions of the metallic particles. The HRS light was separated from its linear counterpart by a 3 nm bandwidth interference filter and a monochromator and then detected with a cooled photomultiplier tube, and the pulses were counted with a photon counter. The fundamental input beam was linearly polarized, and the input angle of polarization was selected with a rotating half-wave plate. In all experiments reported, the polarization state of the harmonic light was vertical. Gold nanorods are known to possess strong two-photon luminescence (TPL) [19,41]. To avoid TPL contributions from HRS signal, we have used the following steps: 1) We have used gold nanorods of aspect ratios 2.5 and 2.7, whose λ_{max} is 200 nm far from the excitation wavelength. Our experiments indicate that in case of 860 nm excitation, TPL signal can be observed for nanorods with aspect ratio between 3.3 - 5.2. 2) We have used 3 nm interference filter in front of PMT, to make sure that only second harmonic signal is collected by PMT.

3. Results and Discussion

3.1. NLO Properties of Gold Nanorods and Evidence for Multipoles

To understand whether the two photon scattering intensity at 430 nm light is due to second harmonic generation, we performed power dependent as well as concentration dependent study. **Figure 3** shows the output signal intensities at 430 nm from ss-DNA absorbed gold nanoparticles at different powers of 860 nm incident light. A linear nature of the plot implies that the doubled light is indeed due to the HRS signal.

Figure 4 shows $\log(I_{2\omega})$ vs. $\log(I_{\omega})$ plot. A linear nature of the plot with slope 1.90 also supports that the HRS signal is due to the second harmonic light. The intensity I_{HRS} of the hyper-Rayleigh signal from an aqueous solution of gold nanorods can be expressed as,

$$I_{HRS} = G \left(N_w \beta_w^2 + N_{nano} \beta_{nano}^2 \right) I_{\omega}^2 e^{-N} \text{nano}_{2\omega}^{\epsilon} l \quad (1)$$

where G is a geometric factor, N_w and N_{nano} the number of water molecules and gold nanorods per unit volume,

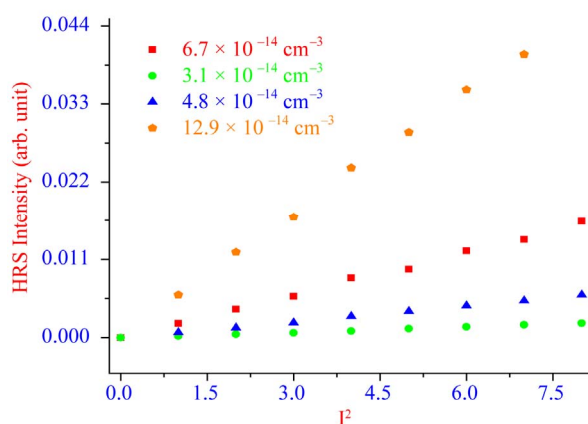


Figure 3. Power dependence of HRS intensity at different concentration of gold nanorods.

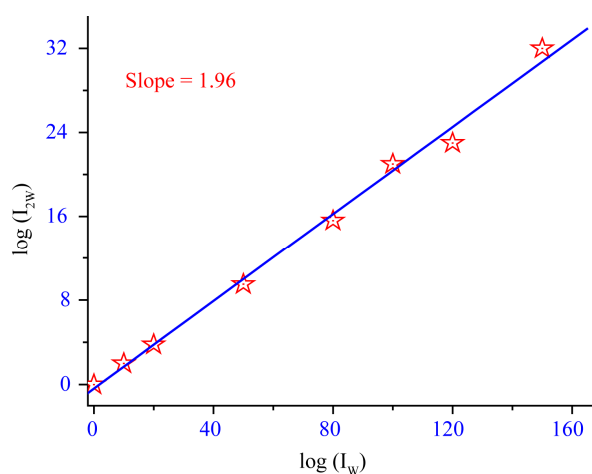


Figure 4. Excitation power dependence of the detected HRS signal from gold nanorod solution (excitation wavelength was 860 nm).

β_w and β_{nano} are the quadratic hyperpolarizabilities of a single water molecule and a single gold nanorod, $\epsilon_{2\omega}$ is the molar extinction coefficient of the gold nanorod at 2ω , l is the path length and I_{ω} the fundamental intensity. The exponential factor accounts for the losses through absorption at the harmonic frequency.

To extract absolute values of the hyperpolarizabilities, the normalized intensities were normalized again with para-nitro aniline (pNA) in methanol. By using $\beta_w = 0.56 \times 10^{-30}$ esu, as reported in the literature, we have found out $\beta_{nano} = 3.8 \times 10^{-24}$ esu for 80 nm gold nanorod and 4.2×10^{-24} esu for DNA adsorbed gold nanorod, which is about 3 - 4 orders of magnitude higher than the β values reported for the best available molecular chromophores [21-27,37] and 1 - 2 orders of magnitude higher than the β value reported for gold nanoparticles [6,22,38-39]. This higher β values for nanorod compared to nanosphere can be due to several facts and these are 1) The presence of $\{110\}$ facets, which is not present in nanospheres, is

known to have strong absorption energies; 2) the surface electromagnetic field of rods is the highest compared to other shapes due to the rod's high curvatures (called "the lightning rod" effect [40]), 3) the presence of multipoles and 4) possibility of single photon resonance enhancement. The optical responses of particles that are small compared to the wavelength can be described usually in the framework of electric-dipole approximation. However, when the particle size approaches the wavelength, the dipolar picture may no longer provide a complete description, and higher multipolar interactions should be considered. Multipoles can arise by two different ways and these are 1) from the light matter interaction Hamiltonian, corresponding to microscopic multipole moments, and 2) according to Mie's scattering theory [41]. Standard Mie's theory is based on dipolar interaction, and multipoles arise from the size and retardation effects. Since there is a center of inversion in nanorod, the HRS intensity arising from gold nanorod cannot be due to electric dipole contribution. At the microscopic scale, the breaking of the centrosymmetry is required for the harmonic generation process at the surface of the particle. Considering the size of a nanorod, the approximation that assumes that the electromagnetic fields are spatially constant over the volume of the particle is not suitable anymore. Higher orders of the electromagnetic field's spatial expansion must be incorporated into the description. As a result, the total nonlinear polarization consists of different contributions such as multipolar radiation of the harmonic energy of the excited dipole and possibly of higher multipoles. The HRS intensity therefore also consists of several contributions. The first one is the electric dipole approximation, which may arise due to the defects in nanorods. This contribution is actually identical to the one observed for any non-centrosymmetrical point-like ob-

jects such as efficient rod-like push-pull molecules. This electric dipole nature presents two lobes oriented along the $0^\circ - 180^\circ$ axis. The second contribution is multipolar contribution like electric quadrupole contribution. This contribution is very important when the size of the particle is no longer negligible when compared to the wavelength.

This contribution pattern shows four lobes (as shown in **Figure 5**) oriented on the 45° , 135° , 225° , and 315° axes when the vertically polarized harmonic output is considered. **Figure 5** demonstrates the polar plots of the HRS intensity vertically polarized as a function of the angle of polarization of the fundamental incoming beam for two types of gold nanorods: 1) 20 nm diameter gold nanoparticle, 2) 120 nm length and 45 nm width gold nanorods. Our experimental results show clearly four-lobe pattern for gold nanorods and two-lobe pattern for gold nanoparticles which infers the origin of the very high HRS light is due to the presence of both dipolar and quadrupolar contributions. For our gold nanoparticle, the ratio between the length of the particles and the wavelength of the fundamental beam is only $3/16$, which is too large to neglect the retardation effect. This four-lobe pattern is not regular as demonstrated by the size inequality between the lobes. In particular, the lobes at 45° and 225° are larger than the ones collected at 135° and 315° . These deviations from the perfect polar plot are due to the retardation effects of the electromagnetic fields.

3.2. Sequence Specific HIV-1 Gag Gene DNA Diagnostics

Figure 6 shows how the HRS intensity varies after the addition of target DNA into probe HIV-1 gag-gene DNA ($5'$ -AGAAGATATTTGGAATAACATGACCTGGATG

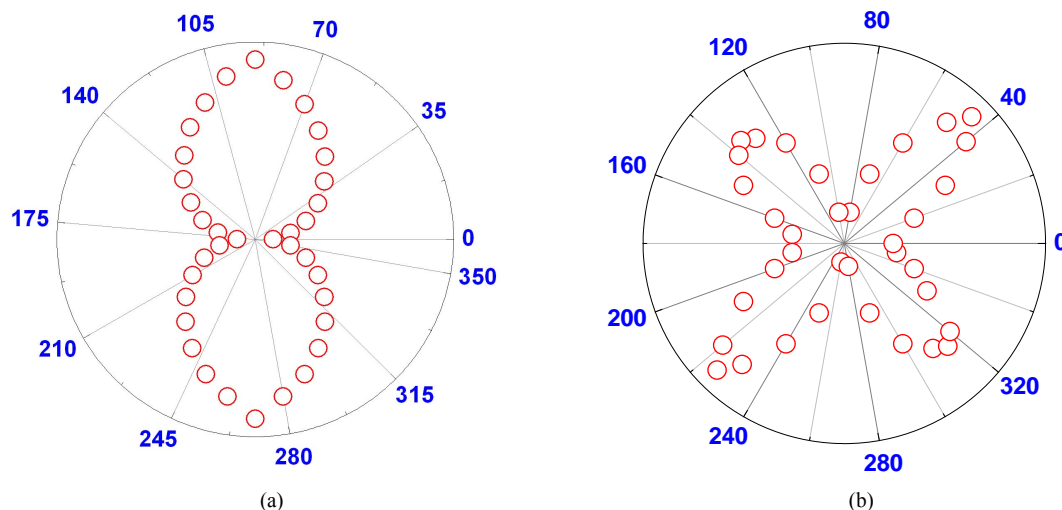


Figure 5. Polar plot of the HRS intensity as a function of the incoming fundamental beam polarization angle from aqueous suspensions of (a) 20 nm gold spherical colloids and (b) 120 nm length and 45 nm width gold nanorods.

CA-3') (400 pM). We observed a very distinct HRS intensity change after hybridization even at the concentration of 100 pico-molar probe ss-DNA. The HRS intensity changes only 10% when we added the target DNA with one base-pair mismatch with respect to probe DNA (as shown in **Figure 6**). Our detection is based on the fact that double and single stranded oligonucleotides have different electrostatic properties as shown in **Scheme 1**.

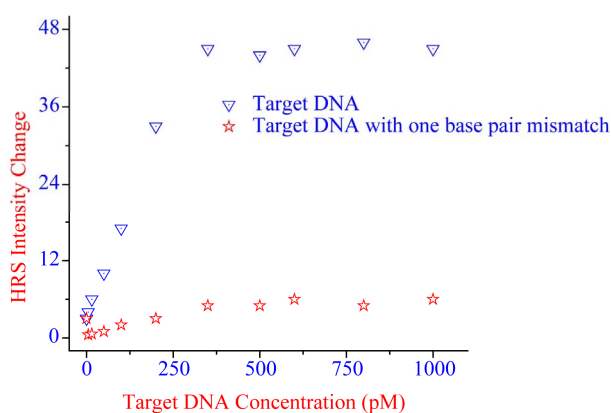
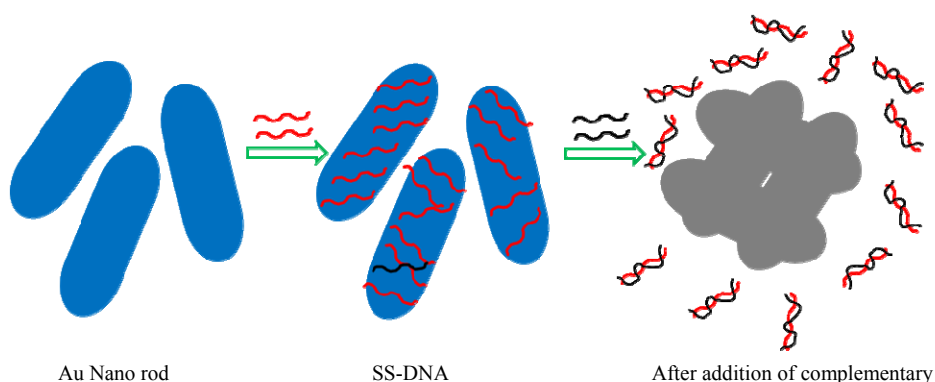


Figure 6. Plot of HRS intensity change vs. target DNA {exact complementary of HIV-1 gag-gene DNA (5'-AGAAG-ATATTTGGAATAACATGACCTGGATGCA-3' and one base pair mismatch} concentration in pico molar level.

When DNA is adsorbed onto the nanorod, due to conformationally flexible backbone of a single-stranded DNA, a favorable conformation for the adsorbed oligos is an arch-like structure, in which both the 3'- and 5'-ends are attached to the particle. Since the ds-DNA cannot uncoil sufficiently like ss-DNA to expose its bases toward the gold nanorods, repulsion between the charged phosphate backbone of ds-DNA and negatively charged ions from the gold nanorods surface dominates the electrostatic interaction, which does not allow ds-DNA to adsorb onto gold nanorods.

In fact ssDNA adsorbs onto the gold whereas dsDNA does not adsorb, can be seen through the effects of adding complementary DNA to solutions containing dye-tagged ssDNA adsorbed onto gold nanorods. Upon hybridization, the double-strand (ds) DNA is no longer adsorbed onto the gold nanorods and the fluorescence of the attached dye persists (as shown in **Figure 2(a)**).

As soon as the ds-DNA separated from gold nanorod, a second effect, aggregation of gold nanorod has been observed as evidenced by TEM image (**Figure 7**), which has been further confirmed by absorption spectroscopic studies (**Figure 8(A)**). This is due to the screening effect of the salt, which minimizes electrostatic repulsion between the oligonucleotide-modified particles, allowing



Scheme 1. Schematic representation of gold nanorod based DNA hybridization process.

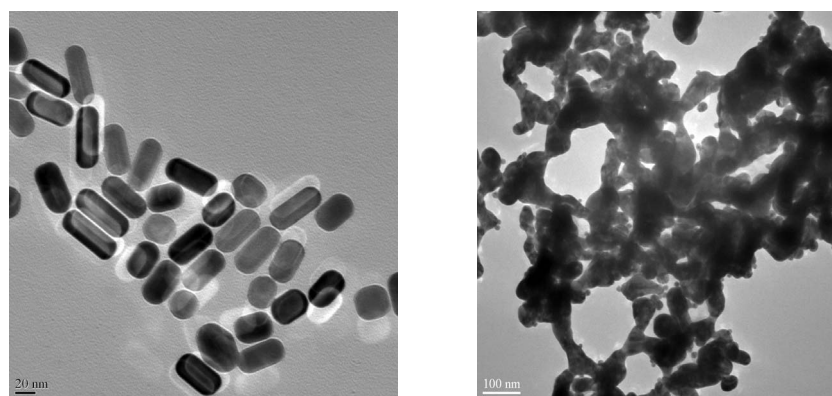


Figure 7. TEM images of Nanorods before and after hybridization.

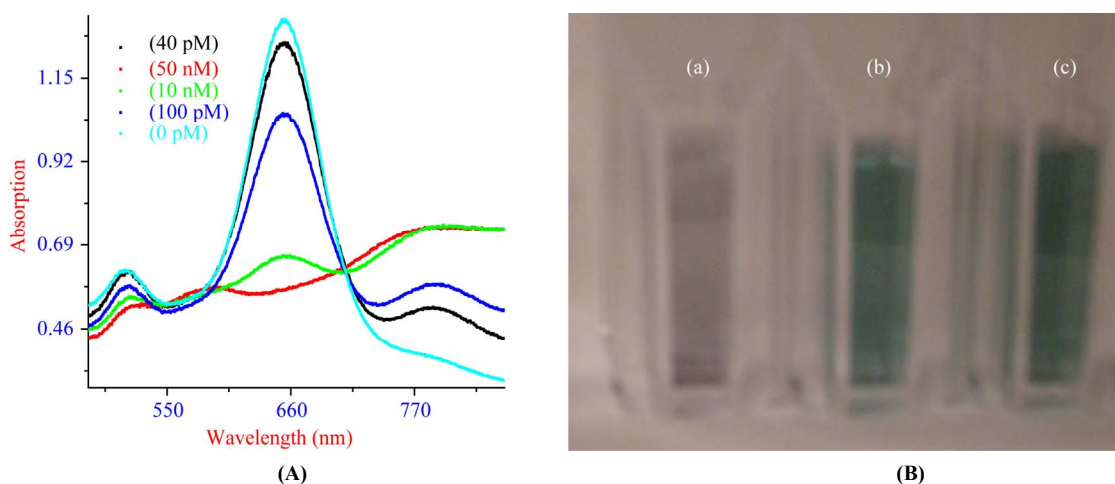


Figure 8. (A) Absorption profile of DNA coated Au nanorods before and after hybridization with different concentrations of probe DNA; (B) Colorimetric change upon addition of (a) 10 nM; (b) 100 pM and (c) 0 pM probe DNA.

more hybridization events to take place, leading to more linked particles and hence larger damping of the surface plasmon absorption of Au nanorod surfaces. We also noted that though the HRS intensity changes about 19 times even at the concentration of 100 pM probe DNA, the visible color changes (as shown in **Figure 8(B)**) can be observed only after the addition of 10 nano-molar complementary DNA, which indicates that our HRS assay is about 2 orders of magnitude more sensitive than the usual colorimetric technique.

After hybridization, the HRS intensity change can be due to several factors and these are as follows: 1) Since after hybridization, aggregation takes place, nanorod loses the center of symmetry and as a result, one can expect significant amount of electric dipole contribution to the HRS intensity. Since electric dipole contributes several times higher than that of multipolar moments, we expect the HRS intensity increases with aggregation. 2) When target DNA with complementary sequence is added to the probe DNA, a clear colorimetric change is observed due to the aggregation as shown in **Figure 8(A)** (absorption maximum changes from 697 nm to 955 nm). A two-level model that has been extensively used for donor-acceptor NLO chromophores can be used to explain the difference of first order non-linearity due to the change in color of nanorods. According to the two-state model [42],

$$\beta^{\text{two state}} = \frac{3\mu_{eg}^2 \Delta\mu_{eg}}{E_{eg}^2} \cdot \frac{\omega_{eg}^2}{(1 - 4\omega^2/\omega_{eg}^2)(\omega_{eg}^2 - \omega^2)} \quad (2)$$

static factor dispersion factor

where μ_{eg} is the transition dipole moment between the ground state $|g\rangle$ and the charge-transfer excited state $|e\rangle$, $\Delta\mu_{eg}$ is the difference in dipole moment and E_{10} is the transition energy. As the color changes, the λ_{max} changes from 697 nm to 955 nm, β should change tremendously

and as a result HRS intensity changes. 3) The single photon resonance enhancement factor is much larger for nanorod aggregates due to the closeness of λ_{max} to the fundamental wavelength at 860 nm. This resonance enhancement should increase HRS intensity. 4) Since size increases tremendously with aggregation, the HRS intensity should increase with the increase in particle size.

To understand how the HRS intensity increases with aggregation, we have performed HRS experiment on pure gold nanorod solution with and without addition of NaCl. **Figure 9** shows how the absorption spectra change as well as HRS intensity increases with NaCl concentration. Our experiment indicates that the HRS intensity enhanced by a factor of 35 as compared to the HRS signal of the pure gold nanorod solution, then slightly decreased and finally saturated at higher NaCl concentration. The enhancement factor is about the same for pure gold nanorod and DNA adsorbed gold nanorod after hybridization.

For genomic analysis, it is desirable to detect specific sequences on much longer HIV DNA targets. To examine ability of our assays to quantify naturally occurring nucleic acid sequences, the HIV *gag* gene was used as a model system. Complementary DNA sequences matching a region found within the nucleocapsid portion of the HIV *gag* gene were tagged with gold nanorod and used as a probe.

86, 115, 142 and 185-bp fragments from the *gag* region of HIV-1 DNA was used as target. **Figure 10** represents the results of proof-of-principle experiments for detecting matches to sequences on long targets, only limitation is that the hybridization process is slow due to the slow adsorption process of long ss-DNA sequence on gold nanoparticle. Although large portions of the target remain single stranded and will presumably have the electrostatic properties of ss-DNA, we have no difficulty using the

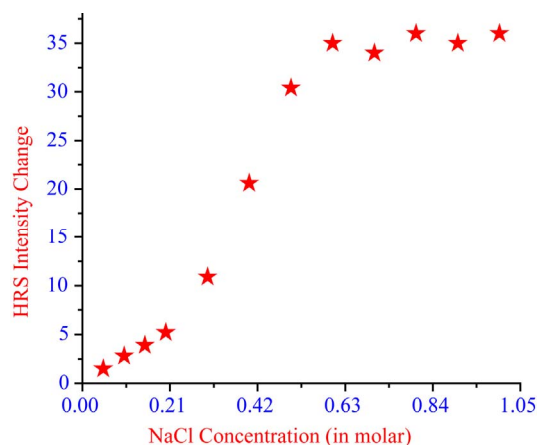


Figure 9. Plot of HRS intensity from gold nanorod vs. different concentration of NaCl.

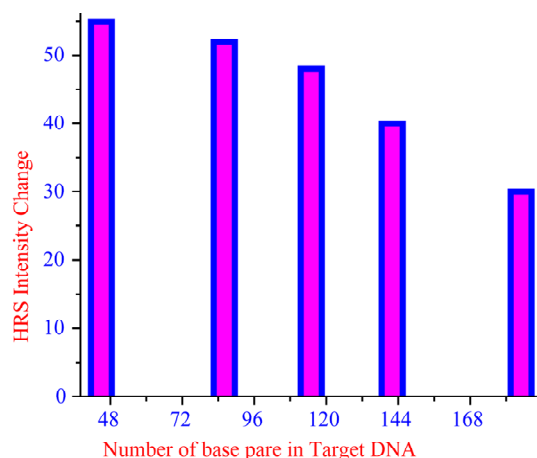


Figure 10. Plot of HRS intensity change as a function of number of base pairs of target *gag* region of HIV-1 DNA.

assay to determine whether these long targets contain sequences complementary to our short dye-tagged probes. Thus, our technique is most practical when short dye-tagged probes (≈ 45 mers) are used.

4. Conclusions

In conclusion, in this manuscript, we have demonstrated for the first time a label free, highly sensitive and sequence-specific HRS assay for HIV *gag* gene DNA sequence recognition in 100 pico-molar level. For a 145-mer oligonucleotide probe, a 100 pM solution of target DNA can be detected with excellent discrimination against single-base mismatches. We provide experimental evidence for higher multipolar contribution to NLO response of gold nanorods. Our HRS assay will have several advantages and these are: 1) one can use unmodified protein and DNA to probe them in solution by the HRS technique; 2) it can be two orders of magnitude more sensitive than the usual colorimetric technique; 3)

single base-pair mismatches are easily detected. The methods and principles presented here can be applied to *in-vitro*-selected aptamers for recognizing a wide range of analytes such as small organic molecules and divalent cations. These nanorod-based HRS probes offer unique advantages and capabilities that are not available from traditional molecular systems. It is probably possible to improve the HRS intensity by several orders of magnitudes by choosing proper materials and detection systems.

5. Acknowledgements

The author takes opportunity to thank to Department of Applied Sciences, Radha Govind Engineering College, Meerut for their generous support and Department of Physics, Banaras Hindu University for providing their experimental facility. I also thank to reviewers Prof. S. B. Rai and others whose valuable suggestions improve the quality of the manuscript.

REFERENCES

- [1] P. Alivisatos, "The Use of Nanocrystals in Biological Detection," *Nature Biotechnology*, Vol. 22, No. 1, 2004, pp. 47-52. [doi:10.1038/nbt927](https://doi.org/10.1038/nbt927)
- [2] E. Katz and I. Willner, "Integrated Nanoparticle-Bio-molecule Hybrid Systems: Synthesis, Properties, and Applications," *Angewandte Chemie International Edition*, Vol. 43, No. 45, 2004, pp. 6042-6108. [doi:10.1002/anie.200400651](https://doi.org/10.1002/anie.200400651)
- [3] J. Xiang, W. Lu, Y. Hu, Y. Wu, H. Yan and C. M. Lieber, "Ge/Si Nanowire Heterostructures as High-Performance Field-Effect Transistors," *Nature*, Vol. 441, 2006, p. 489. [doi:10.1038/nature04796](https://doi.org/10.1038/nature04796)
- [4] J. M. Nam, C. S. Thaxton and C. A. Mirkin, "Nanoparticle-Based Bio-Bar Codes for the Ultrasensitive Detection of Proteins," *Science*, Vol. 301, 2003, pp. 1884-1886.
- [5] X. Gao, Y. Cui, R. M. Levenson, L. W. K. Chung and S. Nie, "In Vivo Cancer Targeting and Imaging with Semiconductor Quantum Dots," *Nature Biotechnology*, Vol. 22, 2004, pp. 969-976. [doi:10.1038/nbt994](https://doi.org/10.1038/nbt994)
- [6] P. C. Ray, "Diagnostics of Single Base-Mismatch DNA Hybridization on Gold Nanoparticles by Using the Hyper-Rayleigh Scattering Technique," *Angewandte Chemie International Edition*, Vol. 45, No. 7, 2006, pp. 1151-1154. [doi:10.1002/anie.200503114](https://doi.org/10.1002/anie.200503114)
- [7] L.-Q. Chu, R. Förch and W. Knoll, "Surface Plasmon-Enhanced Fluorescence Spectroscopy for DNA Detection Using Fluorescently Labeled PNA as 'DNA Indicator'," *Angewandte Chemie International Edition*, Vol. 46, 2007, pp. 4944-4947.
- [8] T. N. Grossmann, L. Röglin and O. Seitz, "Triplex Molecular Beacons as Modular Probes for DNA Detection," *Angewandte Chemie International Edition*, Vol. 46, No. 27, 2007, pp. 5223-5226. [doi:10.1002/anie.200700289](https://doi.org/10.1002/anie.200700289)
- [9] X. Huang, I. H. El-Sayed, W. Qian and M. A. El-Sayed,

- “Cancer Cell Imaging and Photothermal Therapy in the Near-Infrared Region by Using Gold Nanorods,” *Journal of the American Chemical Society*, Vol. 128, No. 6, 2006, pp. 2115-2120. [doi:10.1021/ja057254a](https://doi.org/10.1021/ja057254a)
- [10] X. Huang, I. H. El-Sayed, W. Qian and M. A. El-Sayed, “Cancer Cells Assemble and Align Gold Nanorods Conjugated to Antibodies to Produce Highly Enhanced, Sharp, and Polarized Surface Raman Spectra: A Potential Cancer Diagnostic Marker,” *Nano Letters*, Vol. 7, No. 6, 2007, pp. 1591-1597. [doi:10.1021/nl070472c](https://doi.org/10.1021/nl070472c)
- [11] G. H. Chan, J. Zhao, E. M. Hicks, G. C. Schatz and R. P. Van Duyne, “Plasmonic Properties of Copper Nanoparticles Fabricated by Nanosphere Lithography,” *Nano Letters*, Vol. 7, No. 7, 2007, pp. 1947-1952. [doi:10.1021/nl070648a](https://doi.org/10.1021/nl070648a)
- [12] B. P. Khanal and E. R. Zubarev, “Oxidative Addition of Phenylacetylene through C-H Bond Cleavage to Form the Mg^{II}-Dpp-Bian Complex,” *Angewandte Chemie International Edition*, Vol. 46, No. 27, 2007, pp. 5223-5226. [doi:10.1002/anie.200700289](https://doi.org/10.1002/anie.200700289)
- [13] C.-C. Huang, Z. Yang, K.-H. Lee and H.-T. Chang, “Synthesis of Highly Fluorescent Gold Nanoparticles for Sensing Mercury(II),” *Angewandte Chemie International Edition*, Vol. 46, No. 36, 2007, pp. 6824-6828. [doi:10.1002/anie.200700803](https://doi.org/10.1002/anie.200700803)
- [14] P. C. Ray, A. Fortner and G. K. Darbha, “Gold Nanoparticle Based FRET Assay for the Detection of DNA Cleavage,” *Journal of Physical Chemistry B*, Vol. 110, 2006, pp. 20745-20748.
- [15] T. L. Jennings, M. P. Singh and G. F. Strouse, “Fluorescent Lifetime Quenching near d = 1.5 nm Gold Nanoparticles: Probing NSET Validity,” *Journal of the American Chemical Society*, Vol. 128, No. 16, 2006, pp. 5462-5467. [doi:10.1021/ja0583665](https://doi.org/10.1021/ja0583665)
- [16] P. C. Ray, G. K. Darbha, A. Ray and W. Hardy, “A Gold-Nanoparticle-Based Fluorescence Resonance Energy Transfer Probe for Multiplexed Hybridization Detection: Accurate Identification of Bio-Agents DNA,” *Nanotechnology*, Vol. 18, No. 37, 2007, pp. 375504-375510. [doi:10.1088/0957-4484/18/37/375504](https://doi.org/10.1088/0957-4484/18/37/375504)
- [17] L. Fabris, M. Dante, G. Braun, S. J. Lee, N. O. Reich, M. Moskovits, T.-Q. Nguyen and G. C. Bazan, “A Heterogeneous PNA-Based SERS Method for DNA Detection,” *Journal of the American Chemical Society*, Vol. 129, No. 19, 2007, pp. 6086-6087. [doi:10.1021/ja0705184](https://doi.org/10.1021/ja0705184)
- [18] S. Lal, N. K. Grady, G. P. Goodrich and N. J. Halas, “Profiling the Near Field of a Plasmonic Nanoparticle with Raman-Based Molecular Rulers,” *Nano Letters*, Vol. 6, No. 10, 2006, pp. 2338-2343. [doi:10.1021/nl061892p](https://doi.org/10.1021/nl061892p)
- [19] N. J. Durr, T. Larson, D. K. Smith, B. A. Korgel, K. Sokolov and A. B. Yakar, “Two-Photon Luminescence Imaging of Cancer Cells Using Molecularly Targeted Gold Nanorods,” *Nano Letters*, Vol. 7, No. 4, 2007, pp. 941-945. [doi:10.1021/nl062962v](https://doi.org/10.1021/nl062962v)
- [20] S. Satyabrata and T. K. Mandal, “Tryptophan-Based Peptides to Synthesize Gold and Silver Nanoparticles: A Mechanistic and Kinetic Study,” *Chemistry—A European Journal*, Vol. 27, 2007, pp. 3160-3168.
- [21] J. Strzalka, T. Xu, A. Tronin, S. P. Wu, I. Miloradovic, I. Kuzmenko, T. Gog, M. J. Therien and J. K. Blasie, “Structural Studies of Amphiphilic 4-Helix Bundle Peptides Incorporating Designed Extended Chromophores for Nonlinear Optical Biomolecular Materials,” *Nano Letters*, Vol. 6, No. 11, 2006, pp. 2395-2405. [doi:10.1021/nl062092h](https://doi.org/10.1021/nl062092h)
- [22] I. Russier-Antoine, E. Benichou, G. Bachelier, C. Jonin and P. F. Brevet, “Multipolar Contributions of the Second Harmonic Generation from Silver and Gold Nanoparticles,” *Journal of Physical Chemistry C*, Vol. 111, No. 26, 2007, pp. 9044-9048. [doi:10.1021/jp0675025](https://doi.org/10.1021/jp0675025)
- [23] K. Clays and A. Persoons, “Hyper-Rayleigh Scattering in Solution,” *Physical Review Letters*, Vol. 66, No. 23, 1991, pp. 2980-2983. [doi:10.1103/PhysRevLett.66.2980](https://doi.org/10.1103/PhysRevLett.66.2980)
- [24] G. Hennrich, M. T. Murillo, P. Prados, H. Al-Saraierh, A. El-Dali, D. W. Thompson, J. Collins, P. E. Georghiou, A. Teshome, I. Asselberghs and K. Clays, “Alkynyl Expanded Donor-Acceptor Calixarenes: Geometry and Second-Order Nonlinear Optical Properties,” *Chemistry—A European Journal*, Vol. 13, No. 27, 2007, pp. 7753-7761. [doi:10.1002/chem.200700615](https://doi.org/10.1002/chem.200700615)
- [25] S. Kujala, B. K. Canfield and M. Kauranen, “Multipole Interference in the Second-Harmonic Optical Radiation from Gold Nanoparticles,” *Physical Review Letters*, Vol. 98, No. 16, 2007, pp. 167403-167406. [doi:10.1103/PhysRevLett.98.167403](https://doi.org/10.1103/PhysRevLett.98.167403)
- [26] B. J. Coe, J. A. Harris, L. A. Jones, B. S. Brunshwig, K. Song, K. Clays, J. Garin, J. Orduna, S. J. Coles and M. B. Hursthouse, “Hursthouse, Syntheses and Properties of Two-Dimensional Charged Nonlinear Optical Chromophores Incorporating Redox-Switchable cis-Tetraammineruthenium(II) Centers,” *Journal of the American Chemical Society*, Vol. 127, No. 13, 2005, pp. 4845-4859. [doi:10.1021/ja0424124](https://doi.org/10.1021/ja0424124)
- [27] L. Viau, S. Bidault, O. Maury, S. Brasselet, I. Ledoux, J. Zyss, E. Ishow, K. Nakatani and H. Le Bozec, “All-Optical Orientation of Photoisomerizable Octupolar Zinc(II) Complexes in Polymer Films,” *Journal of the American Chemical Society*, Vol. 126, No. 27, 2004, pp. 8386-8387. [doi:10.1021/ja048143z](https://doi.org/10.1021/ja048143z)
- [28] C. A. Mirkin, R. L. Letsinger, R. C. Mucic and J. J. Storhoff, “Emergence of Simple-Cell Receptive Field Properties by Learning a Sparse Code for Natural Images,” *Nature*, Vol. 382, 1996, pp. 607-610. [doi:10.1038/382607a0](https://doi.org/10.1038/382607a0)
- [29] N. J. Durr, T. Larson, D. K. Smith, B. A. Korgel, K. Sokolov and A. Ben-Yakar, “Two-Photon Luminescence Imaging of Cancer Cells Using Molecularly Targeted Gold Nanorods,” *Nano Letters*, Vol. 7, No. 4, 2007, pp. 941-945. [doi:10.1021/nl062962v](https://doi.org/10.1021/nl062962v)
- [30] C. Sonnichsen and A. P. Alivisatos, “Gold Nanorods as Novel Nonbleaching Plasmon-Based Orientation Sensors for Polarized Single-Particle Microscopy,” *Nano Letters*, Vol. 5, No. 2, 2005, pp. 301-304. [doi:10.1021/nl048089k](https://doi.org/10.1021/nl048089k)
- [31] P. K. Jain, S. K. Lee, I. H. El-Sayed and M. A. El-Sayed, “Calculated Absorption and Scattering Properties of Gold Nanoparticles of Different Size, Shape, and Composition: Applications in Biological Imaging and Biomedicine,” *Journal of Physical Chemistry B*, Vol. 110, No. 14, 2006,

- p. 7238. [doi:10.1021/jp057170o](https://doi.org/10.1021/jp057170o)
- [32] H. F. Wang, T. B. Huff, D. A. Zweifel, W. He, P. S. Low, A. Wei and J.-X. Cheng, "In Vitro and in Vivo Two-Photon Luminescence Imaging of Single Gold Nanorods," *Proceedings of the National Academy of Sciences USA*, Vol. 102, No. 44, 2005, pp. 15752-15756. [doi:10.1073/pnas.0504892102](https://doi.org/10.1073/pnas.0504892102)
- [33] T. Yamada, Y. Iwasaki, H. Tada, H. Iwabuki, M. Chuah, T. VandenDriessche, H. Fukuda, A. Konodo, M. Ueda, M. Seno, K. Tanizawa and S. Kuroda, "Nanoparticles for the Delivery of Genes and Drugs to Human Hepatocytes," *Nature Biotechnology*, Vol. 21, 2003, pp. 885-890. [doi:10.1038/nbt843](https://doi.org/10.1038/nbt843)
- [34] C. J. Murphy, T. K. Sau, A. M. Gole, C. J. Orendroff, J. Gao, L. Gou, S. E. Hunyadi and T. Li, "Anisotropic Metal Nanoparticles: Synthesis, Assembly, and Optical Applications," *Journal of Physical Chemistry B*, Vol. 109, No. 29, 2005, pp. 13857-13870. [doi:10.1021/jp0516846](https://doi.org/10.1021/jp0516846)
- [35] G. K. Darbha, A. Ray and P. C. Ray, "Gold Nanoparticle-Based Miniaturized Nanomaterial Surface Energy Transfer Probe for Rapid and Ultrasensitive Detection of Mercury in Soil, Water, and Fish," *ACS Nano*, Vol. 1, No. 3, 2007, pp. 208-214. [doi:10.1021/nn7001954](https://doi.org/10.1021/nn7001954)
- [36] V. S. Tiwari, T. Oleg, G. K. Darbha, W. Hardy, J. P. Singh and P. C. Ray, "Non-Resonance SERS Effects of Silver Colloids with Different Shapes," *Chemical Physics Letters*, Vol. 446, No. 1-3, 2007, pp. 77-82. [doi:10.1016/j.cplett.2007.07.106](https://doi.org/10.1016/j.cplett.2007.07.106)
- [37] H. Kang, G. Evmenenko, P. Dutta, K. Clays, K. Song and T. J. Marks, "X-Shaped Electro-optic Chromophore with Remarkably Blue-Shifted Optical Absorption. Synthesis, Characterization, Linear/Nonlinear Optical Properties, Self-Assembly, and Thin Film Microstructural Characteristics," *Journal of the American Chemical Society*, Vol. 128, No. 18, 2006, pp. 6194-6205. [doi:10.1021/ja060185v](https://doi.org/10.1021/ja060185v)
- [38] P. Galletto, P. F. Brevet, H. H. Girault, R. Antoine and M. Broyer, "Enhancement of the Second Harmonic Response by Adsorbates on Gold Colloids: The Effect of Aggregation," *Journal of Physical Chemistry B*, Vol. 103, No. 41, 1999, pp. 8706-8710. [doi:10.1021/jp991937t](https://doi.org/10.1021/jp991937t)
- [39] J. P. Novak, L. C. Brousseau, F. W. Vance, R. C. Johnson, B. I. Lemon, J. T. Hupp and D. L. Feldheim, "Nonlinear Optical Properties of Molecularly Bridged Gold Nanoparticle Arrays," *Journal of the American Chemical Society*, Vol. 122, No. 48, 2000, pp. 12029-12030. [doi:10.1021/ja003129h](https://doi.org/10.1021/ja003129h)
- [40] C. Hubert, A. Rumyantseva, G. Lerondel, J. Grand, S. Kostcheev, L. Billot, A. Vial, R. Bachelot, P. Royer, S.-H. Chang, S. K. Gray, G. P. Wiederrecht and G. C. Schatz, "Near-Field Photochemical Imaging of Noble Metal Nanostructures," *Nano Letters*, Vol. 5, No. 4, 2005, pp. 615-619. [doi:10.1021/nl047956i](https://doi.org/10.1021/nl047956i)
- [41] G. Mie, "Beiträge zur Optik Trüber Medien, Speziell Kolloidaler Metallösungen," *Annalen der Physik*, Vol. 330, No. 3, 1908, pp. 377-445. [doi:10.1002/andp.19083300302](https://doi.org/10.1002/andp.19083300302)
- [42] J. L. Oudar, "Optical Nonlinearities of Conjugated Molecules. Stilbene Derivatives and Highly Polar Aromatic Compounds," *Journal of Physical Chemistry*, Vol. 67, No. 2, 1977, pp. 446-454. [doi:10.1063/1.434888](https://doi.org/10.1063/1.434888)